Journal of Applied Polymer Science

Preparation and Performance Evaluations of Electrospun Poly(ε-caprolactone), Poly(lactic acid), and Their Hybrid (50/50) Nanofibrous Mats Containing Thymol as an Herbal Drug for Effective Wound Healing

Zeinab Karami,[1] Iraj Rezaeian,[1] Payam Zahedi,[1] Mohammad Abdollahi[2]

[1]School of Chemical Engineering, College of Engineering, University of Tehran, P. O. Box 11155-4563, Tehran, Iran

[2]Faculty of Pharmacy, Pharmaceutical Sciences Research Center, and Endocrinology and Metabolism Research Center, Tehran University of Medical Sciences, Tehran, Iran

Correspondence to: I. Rezaeian (E-mail: rezaeian@ut.ac.ir)

ABSTRACT: The use of herbal drugs as biocompatible and nontoxic drugs without special side effects in wound dressings are highly favored compared to that of chemical and synthetic drugs. In this study, the properties and performance of electrospun poly(ε-caprolactone) (PCL), poly(lactic acid) (PLA), and their 50/50 hybrid nanofibrous mats containing the herbal drug thymol (1.2% v/v) as wound dressings were investigated. The optimized solution concentrations of PCL (12% w/v) and PLA (3% w/v) in chloroform/dimethylformamide (7:3) for electrospinning were determined with viscometry and scanning electron microscopy studies to obtain smooth and beadless nanofibers. The results of the drug-release behavior along with swelling tests showed that the electrospun 50/50 PCL/PLA hybrid nanofibers had the highest level of drug release (∼ 72%) compared with the PCL and PLA nanofibrous samples. The release kinetics of thymol from PCL, PLA, and 50/50 PCL/PLA hybrid nanofibrous mats were studied by the Peppas equation and the zero-order, first-order, Higuchi, and Hixon–Crowell models. Antibacterial evaluations showed that the electrospun 50/50 PCL/PLA hybrid nanofibrous samples containing thymol had satisfactory effects on *Staphylococcus aureus* compared with *Escherichia coli* bacteria during the treatment periods. *In vivo* rat wound-healing and histological performance observations of thymol-loaded 50/50 PCL/PLA nanofibrous mats, the commercial wound dressing Comfeel Plus, and gauze bandages (control) after 14-day post-treatment periods were evaluated. The results reveal that the electrospun 50/50 PCL/PLA hybrid nanofibers containing thymol had a remarkable wound-closure percentage of about 92.5% after a period of 14 days. Finally, the crystallinity and thermal behavior of the electrospun 50/50 PCL/PLA hybrid nanofibrous mats with and without thymol were studied by differential scanning calorimetry. © 2012 Wiley Periodicals, Inc. J. Appl. Polym. Sci. 129: 756–766, 2013

KEYWORDS: biocompatibility; biomedical applications; drug-delivery systems; electrospinning; polyesters

Received 29 August 2012; accepted 2 October 2012; published online 27 November 2012

DOI: 10.1002/app.38683

INTRODUCTION

Since ancient times, different kinds of materials have been used for effective wound healing. Materials such as milk, herbs, honey pastes, and animal fats have been used as wound-dressing materials.[1,2] Historically, the use of herbal plants and their derivatives have always had special importance and benefits in the wound-closure process. The long-term toxicity and harmful side effects of herbal plants are often insignificant compared to those of synthetic drugs. The main disadvantage of herbal drugs is that they have to be used in higher dosages than synthetic ones. The high amounts of herbal drugs extracted from plants decrease their solubility in water or other chemical solvents. Therefore, in polymer carriers, such as encapsulates, electrospun mats, and casting films, containing herbal drugs, the dissolution of herbal extracts hardly happens. This can even have negative effects on the drug-release behavior. Despite these problems, herbal drugs show great promise for success compared to chemical materials because of their excellent performance in wound treatment.[3]

Although skin damage caused by injuries is somewhat fixable by the body itself, often, depending on the severity of the injury, immediate medical care is required. This issue can emphasize the importance of an appropriate wound dressing, which can protect wounds from contamination and infection and wipe out any

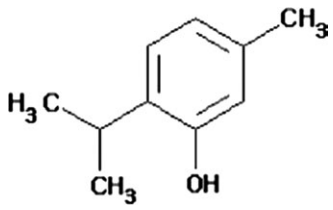

Figure 1. Schematic chemical structure of thymol.

exudation.[4] The purpose of wound-dressing materials are to produce an ideal structure with a high porosity; this acts as a barrier against external agents such as bacteria and fungi and aids in rapid wound healing.[5] To reach this target, materials used as wound dressings must be carefully selected, and their structure should control the water vapor and oxygen transmission rates.[6,7] However, the presence of a small amount of exudate on the wound will develop the healing process and keep the wound surface moist, but additional amounts of exudate must be removed from the wound surface to prevent it from becoming an environment that is susceptible to the growth of bacteria and other microorganisms.[4,8] Some conventional wound dressings, such as the medical absorbent Carbasus or Comfeel Plus pads, are dressings that are used only to cover the wound and do not have any special properties, such as gas permeability or water uptake.[7]

Recently, the use of active components that are placed in wound dressings and directly react with cells or release special chemicals (e.g., antibiotics, growth factors, vitamins, minerals, or silver particles) at the wound site have been developed.[1] On the basis of these active agents for wound healing, polymeric films containing herbal drugs have been used as wound dressings; they can be prepared by different methods, such as film casting and electrospinning processes.[9–15] These drugs are good options for wound healing because of their nontoxicity and high compatibility in the physiological and biological environments. The use of herbs is very common in East Asian countries. For example, in Thailand, curcumin is an active component extracted from turmeric that has antioxidant and anti-inflammatory effects.

To improve the mechanical properties of a wound dressing, Merrell et al.[9] used electrospun poly(ε-caprolactone) (PCL) nanofibrous mats containing curcumin for the healing of diabetic wounds. Their results showed that the PCL nanofibers had a sustained release of curcumin for 72 h and suitable antioxidant activity for oxygen radical absorbance. They also concluded that the curcumin-loaded nanofibers reduced inflammatory induction. The *in vivo* wound-healing capability of the samples was demonstrated by an increased rate of wound closure in a diabetic mice model. The use of *Centella asiatica* extract for healing burned wounds and skin disorders was reported.[10] In another study, Opanasopit et al.[11] examined the release of mangosteen (an antibacterial, antioxidant, and anti-inflammatory agent) from electrospun poly(vinyl alcohol) (PVA) nanofibers.

Thyme oil as an essential oil has many components with different characteristics. Among them, its antimicrobial properties are related to thymol and carvacrol (phenolic components) ingredients, which are conveniently used in mouthwash, soaps, and creams, and their performance has been evaluated by *in vitro* and *in vivo* experiments.[16,17] Figure 1 shows the thymol chemical structure; thymol is the most abundant component in thyme oil. So far, a few research works have investigated the role of thymol-loaded polymer carriers for wound healing. The use of thymol in some polymer processes, such as encapsulation[18] and film casting,[15] have been reported. There have been no reports on the addition of thymol as an antibacterial and proliferative agent into electrospun polymer nanofibrous mats as wound-dressing materials.

The electrospinning process is the only cost-effective method that provides continuous and long fibers with average diameters from micrometers to nanometers. These nanofibrous mats are used in different fields of application, such as tissue engineering,[19] drug-delivery systems,[20,21] wound dressings,[7,22] and medical applications.[19] In the electrospinning process, a melt polymer or polymer solution is pumped into a thin nozzle (Figure 2).[23] The nozzle acts simultaneously as an electrode to create a strong electrical field. Applied voltage causes the formation of a cone-shaped droplet of polymer solution on the tip of a needle, which moves toward the opposite electrode (collector) and becomes thinner during the process. Solvent evaporation occurs in the movement of the polymer solution jet toward the collector and solid fibers with diameters ranging from nanometers to micrometers are deposited onto the collector.

Covering the wounds with electrospun nanofibrous mats has many advantages compared to conventional dressing materials. For example, their high aspect ratio and microporous structure provide the possibility of gaseous exchange and prevent wound from drying; this results in rapid progress in wound healing.[8] It can be concluded that dressings prepared from polymer nanofibrous mats have almost all of the properties expected from good wound-dressing materials for a rapid healing process.

The main purpose of this study was to provide electrospun nanofibrous mats prepared from PCL, poly(lactic acid) (PLA), and 50/50

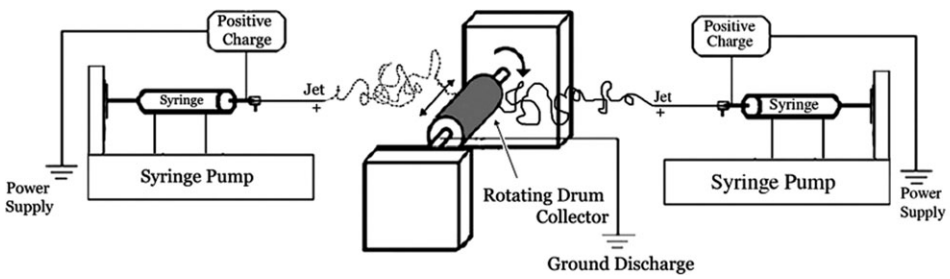

Figure 2. Schematic presentation of the electrospinning process.

hybrid solutions. For the first time, thymol as an active component in the healing process of wounds was added to these nanofibrous samples. The drug-loaded electrospun PLA, PCL, and their 50/50 hybrid nanofibers were evaluated by their *in vitro* drug-release rate and an *in vivo* rat wound model, and their performance in accelerating wound healing was compared with the commercial wound dressing Comfeel Plus and gauze bandages (the control).

EXPERIMENTAL

Materials

Poly(D-lactic acid) (Resomer LR708 grade, inherent viscosity = 5.7–6.5 dL/g) was obtained from Evonik Industries (Darmstadt, Germany). PCL (biodegradable, number-average molecular weight = 70–80 kg/mol) was purchased from Sigma-Aldrich Co. (Pilsburg, The Netherlands). Thymol (an herbal drug and the most important component in thyme oil, density = 0.97 g/cm^3 at 20 °C) was provided from Merck KGaA (Darmstadt, Germany). The polyurethane wound dressing Comfeel Plus was supplied from Coloplast Co. (Hurnlebeek, Denmark). All of the other chemicals were analytical-reagent grade and were used without further purification.

Sample Preparation

To prepare neat electrospun PCL and PLA nanofibrous mats, weighed PCL and PLA granules were dissolved in a mixture of chloroform and dimethylformamide (DMF; 7:3) as the solvent system and were stirred for about 1 h at room temperature. To prepare nanofibrous samples containing the drug, the weighed polymers and thymol were dissolved in chloroform and DMF, respectively, and then, the mixture was stirred for about 30 min. Hybrid nanofibrous mats of 50/50 PCL/PLA were prepared with a syringe containing PCL and the drug and a second syringe containing PLA and the drug.

According to the previous conditions, a simultaneous injection from two separate syringes, the electrospinning process was carried out at previously determined optimum conditions.[23] The spun nanofibrous mats were collected on sterile aluminum foil. The electrospinning device used for the preparation of the samples was a model eSpinner NF-CO EN/II from Asian Nanostructures Technology Co. (Tehran, Iran). The electrospinning conditions for PCL, PLA, and their 50/50 hybrid nanofibrous samples were as follows: flow rate = 0.7 mL/h, applied voltage = 15 kV, distance between the needle tip and the collector = 12 cm, and needle gauge = 0.7 mm. To achieve a fully dried electrospun nanofibrous sample and to ensure complete evaporation of the organic solvents from the spun fibers, the samples were then dried at room temperature for about 12 h at a relative humidity of 32% until a constant weight was attained.

Characterization of the Samples

Viscometry. To determine the optimum viscosity and concentration values of the PCL and PLA solutions in chloroform/DMF (7:3), a digital Brookfield viscometer (model DVII+Pro) (Middleboro, MA, United States) was used at room temperature. The different concentrations of the PLA and PCL solutions for viscometry measurements were 1–5 and 11–15% w/v, respectively. The average of at least five measurements with a standard deviation of less than 5% was recorded.

Morphological Studies. The electrospun nanofibrous samples on aluminum foil were coated with a thin layer of gold by a Bio-Rad 5200 auto sputter coater (Agar Scientific Ltd., Essex, United Kingdom). The morphology of the electrospun nanofibrous samples were observed by scanning electron microscopy (SEM; CamScan MV2300, Oxford, United Kingdom) at 2500 and 5000 × magnifications. The mean values of the nanofiber diameters from five different sections were recorded.

Swelling and Weight Loss Investigations. To determine the degree of swelling as an effective parameter in the drug-release mechanism for the nanofibrous samples, the samples were immersed in acetate buffer (pH 5.5 at 37 °C) for 1, 4, 24, and 48 h. The degree of swelling and the weight loss percentage of the samples were calculated according to eqs. (1) and (2):

$$\text{Degree of swelling}\,(\%) = \frac{M - M_d}{M_d} \times 100 \quad (1)$$

$$\text{Weight loss}\,(\%) = \frac{M_i - M_d}{M_i} \times 100 \quad (2)$$

where M is the weight of the swollen samples that were drip-dried by filter paper, M_d is the weight of the dried samples in an oven at 40 °C until a constant weight was obtained, and M_i is the initial weight of the samples.

Study of the Drug-Release Rate from the Samples Containing Thymol. To measure the release rate of thymol from the electrospun nanofibrous mats, 10 × 30 cm^2 samples containing 0.058 g of thymol were immersed in 40 mL of acetate buffer solution (pH 5.5 at 37 °C) with a constant stirring rate for a period of 48 h.

An ultraviolet–visible spectrometer (model CECIL CE 7250, 7000 SERIS, Cecil Instruments Ltd., Cambridge, United Kingdom) was used to determine the amount of drug released. The maximum wavelength of thymol in DMF was about 289 nm. To plot the calibration curve (Figure 3) on the basis of the Beer–Lambert equation, thymol solutions with different concentrations of 0.2–2% v/

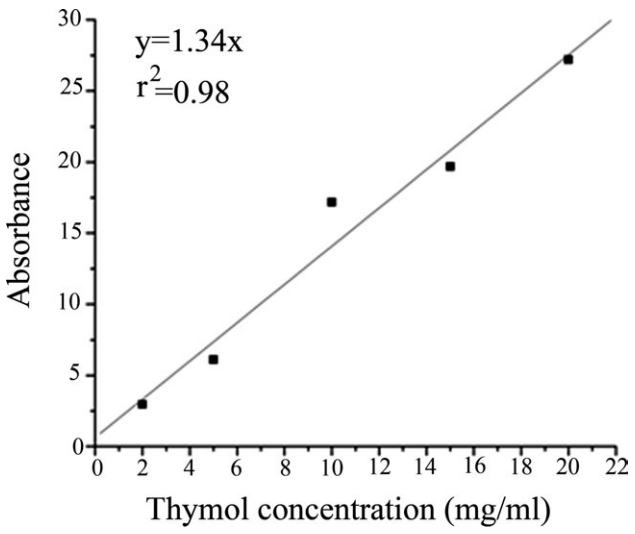

Figure 3. Thymol calibration curve according to the Beer–Lambert equation obtained by ultraviolet–visible spectroscopy.

v in DMF[15] were prepared, and their UV absorptions at the determined wavelength were measured. The calibration equation with an r^2 value of about 0.98 was calculated as follows:

$$A = \varepsilon \times 1 \times c = 1.34c \quad (3)$$

where A is the absorption, c is the thymol concentration, l is the distance the light travels through the material, and ε is the extinction coefficient. The molar extinction coefficient for thymol in DMF was found to be 9.019 L/mol for 1 cm of a linear Beer–Lambert curve.

Analysis of the Drug-Release Kinetics. For the evaluation of the drug-release kinetics and the determination of its mechanism in all of the samples, the Peppas–Korsmeyer equation was used:

$$\frac{M_t}{M_\infty} = Kt^n \quad (4)$$

where M_t is the cumulative amount of drug released at time t, M_∞ is the initial drug loading, K is a constant characteristic of the drug–polymer system, and n is the diffusion exponent, which suggests the nature of the release mechanism. In addition to Fickian theory, four more models were used to further analyze the drug-release profile, including the zero-order, first-order, Higuchi, and Hixon–Crowell models.[24] These model equations are listed as follows:

$$\text{Zero-order}: \ Q_t = Q_0 + K_0 t \quad (5)$$

$$\text{First-order}: \ \text{Ln}\, Q_t = \text{Ln}\, Q_0 + K_1 t \quad (6)$$

$$\text{Higuchi}: \ Q_t = K_H t^{1/2} \quad (7)$$

$$\text{Hixon} - \text{Crowell}: \ Q_0^{1/3} - Q_t^{1/3} = K_s t \quad (8)$$

where Q_t is the amount of drug dissolved in time t, Q_0 is the initial amount of drug in the solution (most of the time, $Q_0 = 0$), K_0 is the zero-order release constant, K_1 is the first-order release constant K_H is the Higuchi dissolution constant, and K_S is a constant incorporating the surface–volume relation.

Evaluation of the Antibacterial Properties of the Electrospun Mats. The antibacterial properties of the electrospun mats with and without thymol were carried out against *Staphylococcus aureus* (Gram-positive) and *Escherichia coli* (Gram-negative) bacteria. The antimicrobial activities of the electrospun mats were studied by the disc diffusion method. This method was performed in a Luria–Bertani medium solid agar Petri dish.[25] The samples were cut into disc shapes 1 cm in diameter, sterilized under UV light for 2 h, and placed on *E. coli* and *S. aureus* cultured agar plates. Then, they were incubated for 24 h at 37 °C, and the inhibition zones were recorded.

***In Vivo* Wound-Healing and Histological studies.** Male Wistar rats (375 ± 25 g) were used in this study ($n = 5$). After anesthetization by ketamine (40 mg/kg) and xylazine (15 mg/kg), the hairs on their back were removed with a shaver and depilatory cream. A full-thickness square wound (2 × 2 cm^2) was cut from the back of each rat. Each wound was then covered with cotton gauze, a hybrid electrospun mat containing thymol, and the commercial wound dressing Comfeel Plus. The treated rats were then placed in individual cages, and the healing wounds were observed daily and photographed with a digital camera for a period of 14 days. The degree of wound healing was expressed as the wound-closure percentage:[26]

$$\text{Wound closure} = \frac{A_t - A_0}{A_0} \times 100 \quad (9)$$

where A_0 and A_t are the initial wound area and the wound area at time t, respectively.

For histological investigations, the healed tissue with adjacent normal skin were excised and fixed in 10% formalin. The excised wound sites fixed in formalin were embedded in paraffin and sectioned at 5 μm. The sections were stained with hematoxylin and eosin for the histological observations of re-epithelialization and granulation.[27]

Differential scanning calorimetry (DSC) Measurements. DSC analysis of the electrospun 50/50 PCL/PLA nanofibrous mats with and without thymol was carried out on a TA Instruments model 2010 (DuPont Co., WA, United States) instrument at a heating rate of 5 °C/min. Before DSC analysis, all of the samples were fully dried in an oven at 40 °C for 24 h and then kept in a desiccator with silica gel. Then, the electrospun samples were sealed in aluminum pans and heated from room temperature to 540 K.

RESULTS AND DISCUSSION

Viscosity Investigations

The concentration and relative viscosity are the most effective factors controlling the nanofiber morphologies. For lower concentrations of polymer solutions in the electrospinning process, the dominant morphologies are those that have beads. Increasing the concentration leads to a substantial decrease in bead formation and produces relatively fine and smooth nanofibers.[28] Figure 4(a,b) shows the relative viscosities of the PCL and PLA solutions at different concentrations in chloroform/DMF (7:3) via the Brookfield viscometer measurements. The results revealed that the viscosity threshold for the PLA and PCL solutions occurred at 2–4 and 11–13% w/v, respectively. These concentrations may have been the optimum ranges for the electrospinning process and led to smooth and beadless morphologies. For further investigation, morphological assessments were carried out until the best polymer solution concentrations were determined.

Morphological Observations of the Samples

Figure 5 and Table I represent the morphologies and average diameters of the electrospun PCL and PLA nanofibers in their three optimum concentrations, as obtained by viscometry measurements. Figure 5(a,d) shows the morphologies of PLA (2% w/v) and PCL (11% w/v), respectively. As shown in this figure, some aggregated spindle-shaped beads were formed, and they were dispersed throughout the nanofibrous samples. The main reason for bead formation was incomplete evaporation of the solvent before the arrival of the polymer solution jet on the collector surface and agglomerate formation.

Applied Polymer SCIENCE

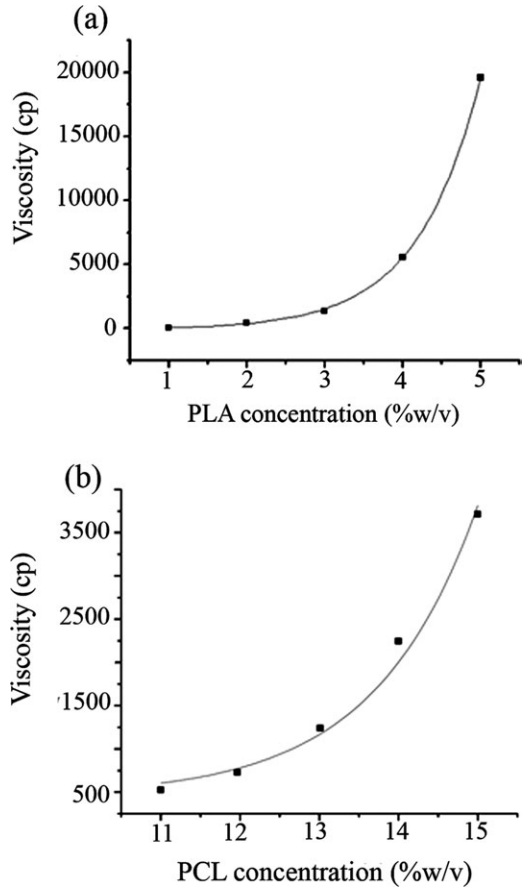

Figure 4. Brookfield viscosity data for (a) PLA and (b) PCL in chloroform/DMF (7:3).

The micrographs in Figure 5(c,f) show the morphologies of the electrospun PLA (4% w/v) and PCL (13% w/v) nanofibers, respectively. In these cases, because of the drastic increase in the viscosities of the polymer solutions, complete solvent evaporation become very hard during the movement of the polymer jet toward the collector, and consequently, wet nanofibers were deposited on the collector.

The following parameters in the morphology of the nanofibrous mats had the most effective control on the drug-release rate:

1. The absence of beads in the nanofibers: The beads could trap portions of the drug and result in a reduction in the drug-release rate.
2. The minimum average diameter of the nanofibers: A reduction in the average diameter of the nanofibers resulted in an increase in the surface-area-to-volume ratio of the nanofibers. Therefore, the tendency of the drug molecules absorbed on the surface of the nanofibers increased remarkably.

On this basis, the best selected samples were PLA (3% w/v) [Figure 5(b)] and PCL (12% w/v) [Figure 5(e)] with average diameters of 356 and 267 nm, respectively.

Figure 6(a–c) shows the electrospun 50/50 PLA/PCL hybrid nanofibrous mats. Figure 6(a) represents the neat 50/50 PLA/PCL hybrid sample with a minimum 373-nm average diameter. Figure 6(b) shows a reduction in the average nanofiber diameter from 373 to 288 nm, which was due to the addition of 1.2% v/v thymol, because thymol acted as a plasticizer and rearranged the polymer chains layers, and this led to a decrease in the viscosity of the polymer solution.[20] Figure 6(c) illustrates the electrospun 50/50 PLA/PCL nanofibrous samples containing the maximum amount of thymol (2.4% v/v).[15] As shown by a comparison of the results obtained in Figure 6(b,c), when the amount of thymol was increased from 1.2 to 2.4% v/v, the processability of the electrospun mats became more difficult because the average diameter of the nanofibers in Figure 6(c) increased remarkably, and the fibers tended to stick together. Consequently, there was no nanofibrous structure, and probably, a filmlike structure was formed. This structure had a negative effect on the drug-release rate. The final conclusion was that thymol as a herbal drug had limited solubility in the electrospun polymer solutions.

Degree of Swelling and Weight Loss Values of the Samples

Figure 7(a,b) shows the swelling degree and weight loss values of the electrospun PLA, PCL, and 50/50 hybrid nanofibrous mats after immersion in an acetate buffer environment for 48 h. On the basis of Figure 7(a), the PLA degree of swelling was lower than those of the other samples; this was due to the higher crystallinity of PLA compared to PCL. Therefore, during the initial hours, the diffusion of the acetate buffer environment into the inner layers of the electrospun PLA nanofibers was more difficult than that into the PCL nanofibers because of the greater number of crystalline regions in PLA. Also, the slope of the swelling curve for the electrospun PLA nanofibers in the initial hours was lower than those of the electrospun PCL and 50/50 PLA/PCL hybrid nanofibers. The degrees of swelling for PLA, PCL, and their hybrid were about 300, 350, and 375%, respectively, after 24 h. Also, the trends observed for the previous samples were about 325, 400, and 380% after 48 h. It seemed that there was no significant difference between the results of PCL and the hybrid nanofibers in both the swelling and weight loss tests. The higher degree of swelling led to a higher diffusion of release medium into the nanofiber layers and, finally, more drug release. With regard to the weight loss, Figure 7(b) shows the results of weight reduction in the nanofibrous samples, and no significant weight loss was observed. Among these samples, the highest amount of weight loss belonged to PCL (0.5%), and PLA had the lowest weight loss (0.35%). PLA had a high crystallinity, and a low diffusion of water molecules was expected from it.

Release of Thymol from the Electrospun Mats

The release rate profiles of thymol from electrospun PCL, PLA, and 50/50 hybrid nanofibrous samples are shown in Figure 8. The electrospun PCL nanomats showed a higher release rate than the PCL/PLA (50/50) and PLA nanofibrous samples. The hybrid nanofibrous mats also showed a drug-release behavior between those of PCL and PLA.

Bimodal release profiles were observed for these three samples. This behavior could be divided into two sections, thymol released before 12 h and that released from 12 to 48 h. The behavior of all of the release profiles for the samples showed a burst and sharp pattern. A high portion of the drug was

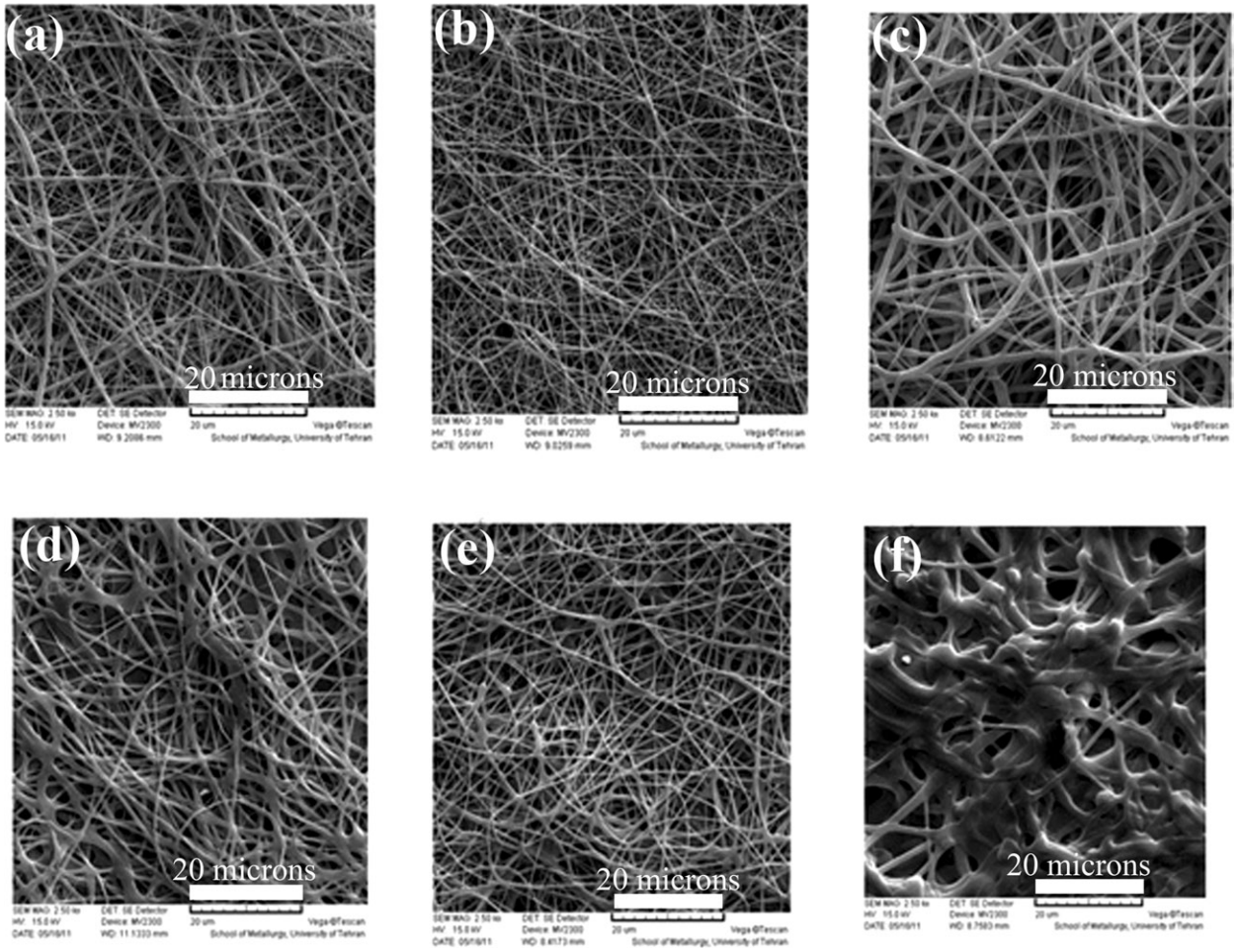

Figure 5. SEM micrographs of the nanofibrous mats prepared from PLA solutions with different concentrations [(a) 2, (b) 3, and (c) 4% w/v] and PCL solutions with different concentrations [(d) 11, (e) 12, and (f) 13% w/v] under constant operating conditions (the scale bars are 20 μm).

released from the nanofibrous samples up to 12 h. After 12 h, a gentle slope and gradual drug release were observed up to 48 h. The burst and rapid release of thymol was related to the adsorption and rapid diffusion of it from the surface of the nanofibrous samples to the release environment due to high aspect ratio of the nanofibers.[28–30] The expedition of drug release could prevent the inflammation of the wound in the initial hours, but generally, a slower release profile is preferable because of the continuous and consecutive release during the presence of wound dressing on the wound. The amounts of released thymol from the electrospun PLA, PCL, and 50/50 hybrid nanofibrous mats were 48.5, 72, and 74% after 24 h and 58.5, 85, and 81% after 48 h, respectively. Therefore, among these three samples, the electrospun PCL/PLA nanofibrous mats were selected as the best because of their slow release and high M_t of the drug after 24 h.

In our previous study,[7] the release behavior of tetracycline hydrochloride from electrospun PCL, PLA, and their 50/50 blend nanofibrous mats were investigated. The release results show that the electrospun 50/50 PCL/PLA blend nanofibrous samples containing 500 μg/mL tetracycline hydrochloride had the highest amount of release, about 72% after 48 h in phosphate buffer solution (PBS), whereas the highest amount of thymol released from the same polymer system was about 58%. To explain this behavior, it should be remembered the solubility of thymol (0.98 g/mL) in distilled water is less than that of tetracycline hydrochloride (10 g/mL). Consequently, when the drug-loaded electrospun nanofibrous samples were immersed into a buffer environment, tetracycline hydrochloride could easily diffuse out of the polymer matrix and dissolve in the aqueous phase, whereas the dissolution of thymol in the release environment was more limited.

Table I. Average Diameters of the PCL and PLA Nanofibers at Different Polymer Concentrations

Sample	Average diameter (nm)
PCL nanofibers (11% w/v)	358 ± 43
PCL nanofibers (12% w/v)	267 ± 23
PCL nanofibers (13% w/v)	582 ± 38
PLA nanofibers (2% w/v)	404 ± 25
PLA nanofibers (3% w/v)	356 ± 31
PLA nanofibers (4% w/v)	490 ± 32

Applied Polymer SCIENCE

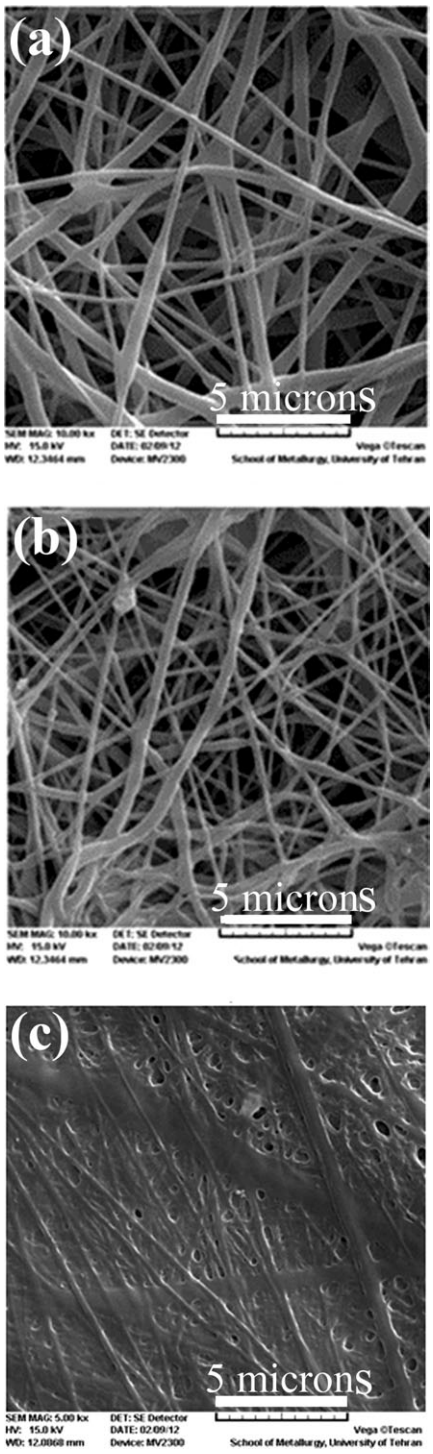

Figure 6. SEM micrographs of the electrospun PCL/PLA (50/50) hybrid nanofibrous mats: (a) neat, (b) 1.2% v/v thymol, and (c) 2.4% v/v thymol (the scale bars are 5 μm).

Analysis of the Thymol Release Kinetics from Electrospun PCL, PLA, and Their 50/50 Hybrid Nanofibrous samples

To investigate the mechanism of thymol released from the nanofibrous samples, the cumulative release profiles were analyzed by the Peppas-Korsmeyer equation and the zero-order, first-order, Higuchi, and Hixon–Crowell models. The regression

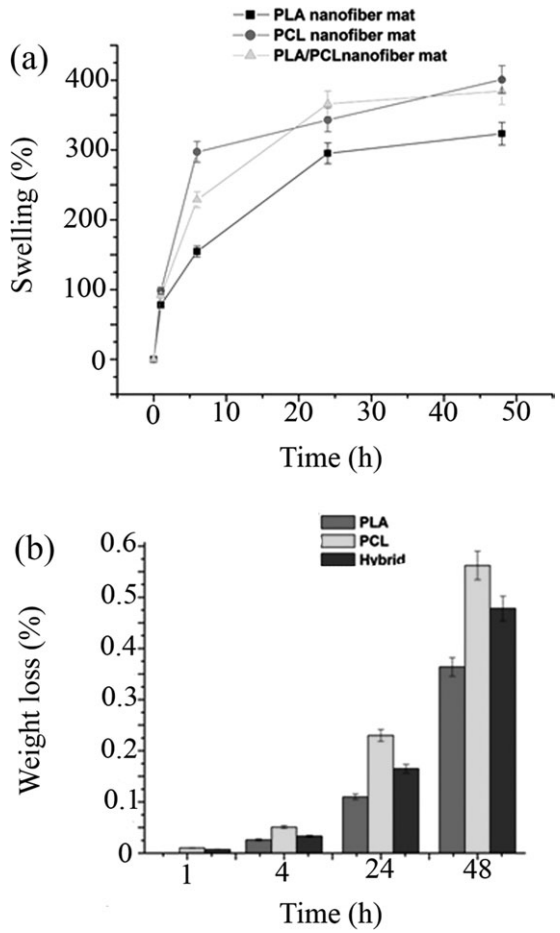

Figure 7. (a) Degree of swelling (%) and (b) weight loss (%) of PCL, PLA, and 50/50 PCL/PLA for the nanofibrous mat samples.

coefficients of the release data fitted by Peppas equation are shown in Table II. The n values related to the drug-loaded samples were about 0.5. Therefore, Fickian diffusion was the dominant mechanism of drug release from the nanofibrous

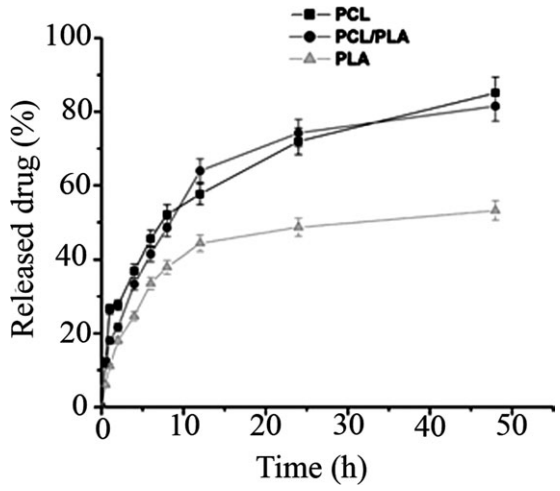

Figure 8. Accumulative release of thymol from the electrospun PLA, PCL, and their 50/50 PCL/PLA hybrid nanofibrous mats versus time.

Table II. Regression Coefficients of the Thymol Released from the Electrospun PCL, PLA, and Their 50/50 PCL/PLA Hybrid Nanofibrous Mats by the Peppas-Korsmeyer Equation

Sample	R^2 ± Standard deviation
PCL nanofibrous mats	0.94 ± 0.01
PLA nanofibrous mats	0.83 ± 0.03
PCL/PLA (50/50) nanofibrous mats	0.97 ± 0.01

$M_t/M_\infty = kt^n$, where $n = 0.5$.

samples to the acetate buffer environment, and the matrix degradation did not have a key role in thymol release.[31]

Table III shows the regression coefficients of thymol release from the nanofibrous samples for different four kinetic models. The high level of initial release was probably due to the diffusion of thymol located on the nanofiber surfaces and its adsorption into the acetate buffer solution; this could be fitted to the Higuchi model. Also, because of the long-time degradation of PLA and PCL, the release mechanism could not be fitted by the Hixon–Crowell model. In addition, the regression coefficients for the different drug-release rates from the samples showed a relative fitness with the zero-order model, which describes the release of a low-soluble drug into the release environment.

Antibacterial Activity Studies of the Electrospun Samples Containing Thymol

Thymol (a component of thyme essential oil) is most applicable for its antibacterial properties. Antibacterial evaluations of the electrospun PCL/PLA (50/50) hybrid nanofibrous mat containing 1.2% v/v thymol against *E. coli* and *S. aureus* were carried out via the disc diffusion method. Figure 9 shows the inhibitory zone formation around the nanofibrous sample discs containing thymol in agar plates of *E. coli* and *S. aureus*. On the other hand, there was no inhibitory zone around the same samples without thymol (control). It should be noted that the inhibitory zone (10.4 mm) against *S. aureus* was larger than the zone (7.8 mm) against *E. coli*. The main reason for this observation was that the activity of thymol against fungi and Gram-positive bacteria is more significant than that against Gram-negative ones.[32] The antibacterial results also confirmed that a 1.2% v/v thymol concentration had a remarkable effect on bacterial growth inhibition, and consequently, the amount of thymol loaded in the electrospun samples was an effective dose for use in *in vivo* rat wound healing.

Wound Closure and Histological Investigations

Figure 10(a,b) shows pictures of the treated wounds and the degree of wound closure in different post-treatment days with gauze (the negative control), the commercial wound dressing Comfeel Plus (the positive control), and the electrospun PCL/PLA (50/50) hybrid nanofibrous mats containing thymol. As shown in these figures, in the wounds treated with gauze bandages, the closure of the wound was not very remarkable compared with those with the other treatments after 14 days [Figure 10(a)]. This was due to the formation of dried clots and the lack of moisture on the surface of the wound. The gauze bandages were stuck to the wound surface, and their removal led to some damage in the regenerated tissues. On the other hand, the wounds covered by Comfeel Plus dressings showed better performance compared with the gauze bandages because they had a high water uptake; this caused a wet environment for the wounds. Consequently, cell growth and fibroblast cell formation happened relatively easily compared to that in a dry wound environment.

The performance of the electrospun PCL/PLA nanofibrous mats containing thymol was somewhat better than that of Comfeel Plus and gauze bandages because the water vapor permeability of the PCL and PLA nanofibers was in the range of 3–4 mg cm^{-2} h^{-1}, but Comfeel Plus was not permeable.[7] The wound-closure percentage of the electrospun PCL/PLA hybrid nanofibrous mats containing thymol was more significant compared with those of the other dressings. As shown in Figure 10(b), the wound-closure percentages of the wounds treated with the electrospun PCL/PLA nanofibrous mats, Comfeel Plus, and gauze bandages were 92.4, 87, and 68%, respectively, at 14 days post-treatment.

Figure 11(a–c) shows the histological photographs of the wounds treated with gauze bandages, Comfeel Plus, and electrospun PCL/PLA (50/50) nanofibrous mats containing thymol at days 7 and 14. At 7 days post-treatment, in the gauze-treated wounds, extensive necrosis, severe inflammatory reactions, and bud tissues beneath the necrosis were observed [Figure 11(a)]. In the Comfeel Plus treated wounds, some granulation tissues, a number of blood vessels, and fibroblast cell formation were observed. Also, the production of collagen fibers and connective fibrils were initiated [Figure 11(b)]. In the case of the wound covered by the electrospun mats containing thymol, an inflammatory state was occurring, and a few portions of epidermis tissue were observed [Figure 11(c)].

At the end of the post-treatment time (day 14), the previous trends were observed again for all of the treated wounds. However, a significant difference was seen in the wound treated with the electrospun PCL/PLA (50/50) hybrid nanofibrous samples containing the drug in terms of granulation tissue formation and re-epithelialization [Figure 11(c)]. However, the formation of epidermis tissue was observed in the wound treated with

Table III. Regression Coefficients of Mathematical Models Fitted to the Release of Thymol from the PCL, PLA, and PCL/PLA (50/50) Nanofibrous Mats

Sample	Zero order	First order	Higuchi	Hixon–Crowell
PCL nanofibers	0.88 ± 0.08	0.74 ± 0.04	0.96 ± 0.03	0.54 ± 0.08
PLA nanofibers	0.77 ± 0.07	0.66 ± 0.09	0.93 ± 0.04	0.58 ± 0.08
PCL/PLA (50/50) nanofibers	0.83 ± 0.09	0.47 ± 0.04	0.96 ± 0.04	0.62 ± 0.08

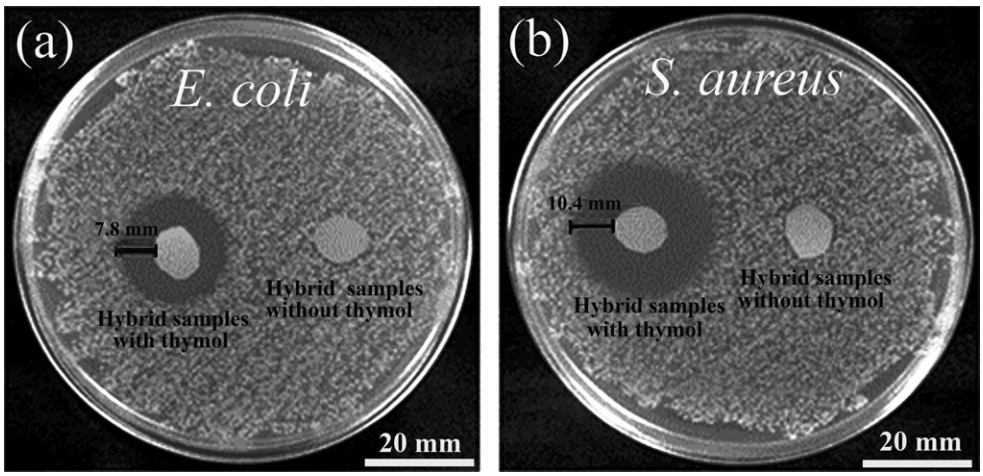

Figure 9. Antibacterial activities of the electrospun PCL/PLA (50/50) hybrid nanofibrous mats containing 1.2% v/v thymol against (a) *E. coli* and (b) *S. aureus* (the scale bars are 20 mm).

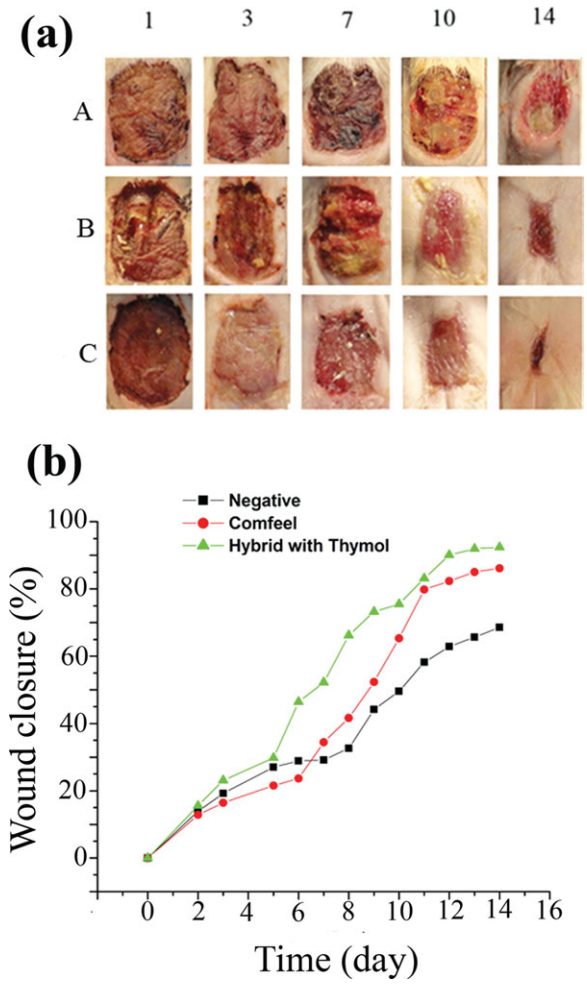

Figure 10. (a) Photographs obtained from wounds covered with (A) gauze, (B) Comfeel Plus, and (C) electrospun PCL/PLA (50/50) nanofibrous mats containing thymol at different times: 1, 3, 7, 10, and 14 days. (b) Degree of closure (%) for wounds treated with gauze, Comfeel Plus, commercial wound dressings on day 14 [Figure 11(b)], but this phenomenon was highly remarkable for the wound covered by the nanofibrous samples with thymol.

Thermal Behavior of the Nanofibrous Samples

Figure 12 shows the DSC peaks for the electrospun PCL/PLA (50/50) hybrid nanofibrous samples with and without thymol. As shown in the diagram for the neat and the drug-loaded samples, the melting point shifted to lower temperatures. This was due to the effect of thymol on the crystals sizes, which led to a reduction in their size and resulted in a lower melting point. On the other hand, the addition of thymol caused imperfect crystal formation in the nanofibrous samples. Electrospinning resulted in a partial alignment of polymer chains; this led to the formation of a cold crystallization phenomenon after the PLA melting peak. As mentioned before, the addition of a drug to the polymer caused rearrangement of the chain layers of the polymer; in this case, the cold crystallization peak became outstanding in the samples containing the drug compared with the neat samples.

CONCLUSIONS

In this study, the wound-dressing properties and performance of nanofibrous mats prepared from PCL, PLA and PCL/PLA (50/50) were evaluated. To improve the properties of these wound-dressing mats, thymol as a component of an herb with anti-inflammatory and antibacterial properties was used. To investigate the performance of these samples, different experiments were carried out. Brookfield viscometer data showed that the optimum concentration ranges for electrospinning of PCL and PLA were 11–13 and 2–4% w/v, respectively. The optimum diameters of PCL and PLA obtained from SEM were about 267 ± 23 and 356 ± 31 nm at 12 and 3% w/v, respectively. The amounts of thymol released after 24 h for PCL, PLA, and their hybrid nanofibers were 72 ± 2, 48.5 ± 1.2, and 74 ± 3.5%, respectively. The results obtained from the swelling and weight loss of the samples were confirmed by the drug-release profiles.

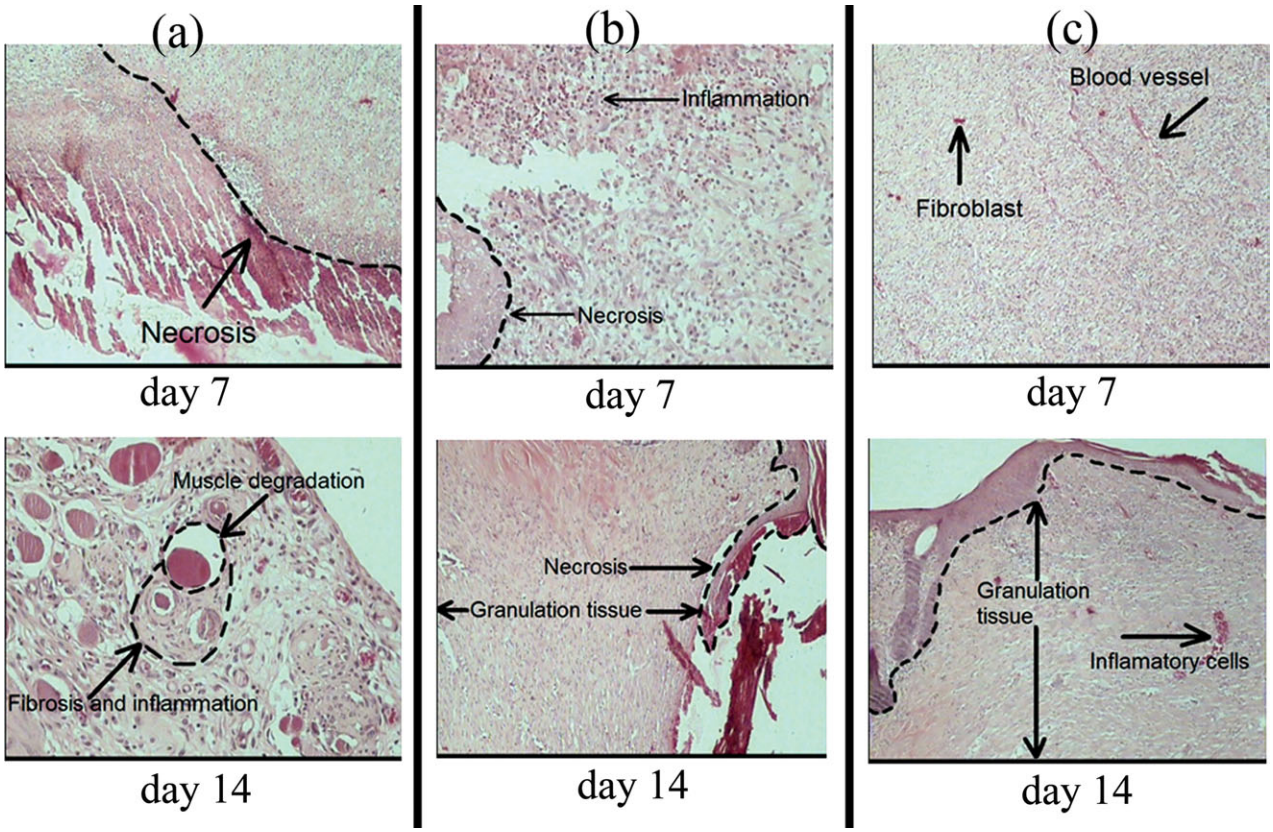

Figure 11. Histological images of wounds covered by (a) gauze, (b) Comfeel Plus, and (c) electrospun PCL/PLA (50/50) nanofibrous samples containing thymol after 7- and 14-day periods. [Color figure can be viewed in the online issue, which is available at wileyonlinelibrary.com.]

In the antibacterial evaluations, the inhibitory zone around the samples for *S. aureus* was significantly larger than that around *E. coli*. The wound-closure studies and their histological observations showed a remarkable performance for the electrospun samples containing thymol compared to the gauze and Comfeel Plus samples. Finally, the effects of thymol on the nanofiber chain layers by DSC were carried out, and their results showed that the addition of the drug had significant effects on the melting point and cold crystallization peak of the polymer nanofibers. In the next step of this research, we will investigate the efficacy of a synthetic drug loaded into hydrophilic and hydrophobic biopolymers and their hybrids separately for healing wounds and compare their *in vitro* and *in vivo* results with thymol as an herbal drug.

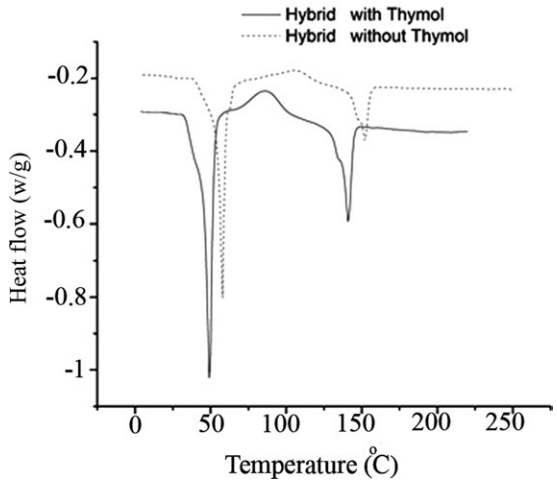

Figure 12. DSC thermograms of the electrospun 50/50 PCL/PLA nanofibrous mats with and without thymol.

ACKNOWLEDGMENT

The authors acknowledge financial support from the Iran National Science Foundation (contract grant number 89001275).

REFERENCES

1. Zahedi, P.; Rezaeian, I.; Ranaei-Siadat, S. O.; Jafari, S. H.; Supaphol, P. *Polym. Adv. Technol.* **2010**, *21*, 77.
2. Ovington, L. G. *Clin. Dermatol.* **2007**, *25*, 33.
3. Seydim, A. C.; Sarikus, G. *Food Res. Int.* **2006**, *39*, 639.
4. Yang, F.; Murugan, R.; Wang, S.; Ramakrishna, S. *Biomaterials* **2005**, *26*, 2603.
5. Robson, M.; Stenberg, B.; Heggers, J. *Clin. Plast. Surg* **1990**, *3*, 485.
6. Ramakrishna, S.; Fujihara, K.; Teo, W. E.; Lim, T. C.; Ma, Z. An Introduction to Electrospinning and Nanofibers; World Scientific: Singapore, **2005**; p 40.

7. Zahedi, P.; Karami, Z.; Rezaeian, I.; Jafari, S. H.; Mahdaviani, P.; Abdolghaffari, A. H.; Abdollahi, M. *J. Appl. Polym. Sci.* **2012**, *124*, 4174.
8. Boateng, J. S.; Matthews, K. H.; Stevens, N. E.; Eccleston, G. M. *J. Pharm. Sci.* **2008**, *97*, 2892.
9. Merrell, J. G.; McLaughlin, S. W.; Tie, L.; Laurencin, C. T.; Chen, A. F.; Nair, L. S. *Clin. Exp. Pharmacol. Physiol.* **2009**, *36*, 1149.
10. Ignatious, F.; Baldoni, J. M. PCT/U.S.Pat. 0102399 (**2001**).
11. Opanasopit, P.; Ruktanonchai, U.; Suwantong, O.; Panomsuk, S.; Ngawhirunpat, T.; Sittisombut, C.; Suksamran, T.; Supaphol, P. *J. Cosmet. Sci.* **2008**, *59*, 233.
12. Casagrande, R.; Georgetti, S. R.; Waldiceu, A.; Verri, W. A., Jr.; Dorta, D. J.; dos Santos, A. C.; Fonseca, M. J. V. *J. Photochem. Photobiol. B* **2006**, *84*, 21.
13. Casagrande, R.; Georgetti, S. R.; Verri, W. A., Jr.; Borin, M. F.; Lopez, R. F. V.; Fonseca, M. J. V. *Int. J. Pharm.* **2007**, *328*, 183.
14. Dias, A. M. A.; Braga, M. E. M.; Seabra, I. J.; Ferreira, P.; Gil, M. H.; de Sousa, H. C. *Int. J. Pharm.* **2011**, *408*, 9.
15. Altiok, D.; Altiok, E.; Tihminlioglu, F. *J. Mater. Sci. Mater. Med.* **2010**, *21*, 2227.
16. Del Nobile, M. A.; Conte, A.; Incoronato, A. L.; Panza, O. *J. Food Eng.* **2008**, *89*, 57.
17. Burt, S. *Int. J. Food Microbiol.* **2004**, *94*, 223.
18. Martins, I. M.; Rodrigues, S. N.; Barreiro, M. F.; Rodrigues, A. E. *Ind. Eng. Chem. Res.* **2011**, *50*, 898.
19. Zhang, Y.; Lim, C. T.; Ramakrishna, S.; Haung, Z. M. *J. Mater. Sci. Mater. Med.* **2005**, *16*, 933.
20. Zamani, M.; Morshed, M.; Varshosaz, J.; Jannesari, M. *Eur. J. Pharm. Biopharm.* **2010**, *75*, 179.
21. Thompson, C. J.; Chase, G. G.; Yarin, A. L.; Reneker, D. H. *Polymer* **2007**, *48*, 6913.
22. Khil, M. S.; Cha, D. I.; Kim, I. S.; Bhattarai, N. B. *J. Biomed. Mater. Res. B* **2005**, *67*, 675.
23. Zahedi, P.; Rezaeian, I.; Jafari, S. H.; Karami, Z. *Macromol. Res.*, to appear. DOI: 10.1007/s13233-013-1064-z.
24. Jannesari, M.; Varshosaz, J.; Morshed, M.; Zamani, M. *Int. J. Nanomed.* **2011**, *6*, 993.
25. Maneerung, T.; Tokura, S.; Rujiravanit, R. *Carbohydr. Polym.* **2008**, *72*, 43.
26. Huang, M. H.; Yang, M. C. *Int. J. Pharm.* **2008**, *346*, 38.
27. Mi, F. L.; Shyu, S. S.; Wu, Y. B.; Lee, S. T.; Shyong, J. Y.; Huang, R. N. *Biomaterials* **2001**, *22*, 165.
28. Kenawy, E. R.; Bowlin, G. L.; Mansfield, K.; Layman, J.; Simpson, D. G.; Sanders, E. H.; Wnek, G. E. *J. Controlled Release* **2002**, *81*, 57.
29. Neamnark, A.; Rujiravanit, R.; Supaphol, P. *Carbohydr. Polym.* **2006**, *66*, 298.
30. Bhardwaj, N.; Kundu, S. C. *Biotechnol. Adv.* **2010**, *28*, 325.
31. Costa, P.; Sousa Lobo, J. M. *Eur. J. Pharm. Sci.* **2001**, *13*, 123.
32. Taepaiboon, P.; Rungsardthong, U.; Supaphol, P. *Eur. J. Pharm. Biopharm.* **2007**, *67*, 387.